AN IR AND FLOW REACTOR STUDY OF CHLOROFORM OXIDATION OVER MANGANESE OXIDES

M.V. GALLEGOS†, G. GARBARINO‡, J.E. COLMAN LERNER†, E. FINOCCHIO‡, G. BUSCA‡, J.E. SAMBETH† and M.A. PELUSO†

† Centro de Investigación y Desarrollo en Ciencias Aplicadas "Dr. Jorge J. Ronco" CONICET CCT La Plata, UNLP, 47 Nº 257 (1900) La Plata, Argentina. jecolman@hotmail.com

‡ Dipartimento di Ingegneria Civile, Chimica e Ambientale, Università di Genova, P.le Kennedy 1, I- 16129 Genova, Italy

Abstract **— A series of manganese base oxides (MnCe, MnZr and MnCeZr) obtained by co-precipitation, were characterized by SBET, XRD, TPR, XPS and studied by FTIR in the oxidation reaction of a typical Cl-VOC such as chloroform, CHCl3. The oxides were compared with a manganese oxide obtained from the recycling of spent batteries (MnOx). In addition, the catalytic combustion of $CHCl_3$ in a fixed-bed reactor was analyzed and the $CHCl_3$ conversion decreased in the order: MnZr > MnOx = MnCeZr >MnCe. In all cases, the conversion is higher than that obtained without a catalyst. The surface Mn^{4+}/Mn^{3+} ratio would favor the decomposition of Cl-VOC. The study of $CHCl_3$ reaction atmosphere by in situ IR reveals that in the absence of catalysts, CCl_4, $COCl_2$, C_2Cl_4 and CH_2Cl_2 were observed. On the other hand, C_2Cl_4 is not formed in the presence of catalysts, although CCl_4 and CH_2Cl_2 were observed and must be avoided.**

Keywords **— manganese, chloroform, Cl-VOC, FTIR**

I. INTRODUCTION

Volatile organic compound (VOCs) emissions, produced from industrial processes, mobile sources, etc., are considered to be severe air pollutants. Catalytic oxidation is one of the most attractive routes for the elimination of VOC emissions (Carabineiro *et al*., 2015). Synthetic manganese based-catalysts have been investigated as supported phase, as support or as catalysts for different VOC oxidation reaction, mainly due to the good activity and stability (Granger *et al.*, 2016). It has been investigated for C3 combustion (Baldi *et al*., 1998), for benzene catalytic oxidation over CuO/MnO_2 (Ahn *et al*., 2017) and oxidation of BTX (Genuino *et al*., 2012), for oxidation of ethanol, methyl ethyl ketone and toluene over Ce-Mn monoliths (Colmen Lerner *et al*., 2016). For a series of oxygenated VOCs $MnOx/Al_2O_3$ have been tested giving rise to good results (Aguero *et al*., 2011). Recently, results on MnOx and MnZnO composite, synthesized from waste alkaline and Zn/C batteries, have been reported for the conversion of ethanol, heptane and toluene, (Gallegos *et al*., 2013 and 2017) showing good catalytic activity. Manganese based catalysts have been investigated also for Cl-VOC by using different model molecules; $MnCuOx/TiO_2$ has been tested for the combustion of chlorobenzene (Belkouch *et al*., 2009), while Ce-Mn has been tested for the oxidation of 1,2-dichloroethane and trichloroethylene (De Rivas *et al*., 2008). Among Cl-VOC, chloroform is of interest since the non-negligible presence in car exhaust, paper mills and in industrial off gases (Jose *et al*., 2018). Chloroform is commonly degraded by incineration (Lou and Chang, 1997), photocatalysis (Rodriguez-Chueca *et al*., 2016), electro-oxidation (Cho *et al*., 2018), etc. Few data on chloroform catalytic oxidation have been found, mainly using Pd/Al_2O_3 (Rossin and Farris, 1993). On the other hand, the possible use of spent batteries as starting point for the production of heterogeneous catalysts will benefit both of a reduced impact avoiding the disposal of batteries with garbage in landfills, in the reduction of a dangerous waste and, consequently, in the reduction of heavy metals pollution in the environment (Biswas *et al*., 2016). Gallegos *et al*. (2017) obtained manganese oxides from spent batteries and observed excellent catalytic performances for ethanol and toluene oxidation. In the same article, the reaction mechanism by FTIR spectroscopy of ethanol and toluene oxidation was also studied. Nevertheless, no literature is found on the reaction mechanism of catalytic chloroform oxidation. The aim of this paper is to investigate the chloroform total oxidation over a manganese base oxides (MnCe, MnZr and MnCeZr) obtained by co-precipitation, and compared to a manganese oxide obtained from spent alkaline batteries. In addition, the reaction mechanism of chloroform oxidation onto the solid was studied by "in situ" FTIR spectroscopy.

II. METHODS

A. Catalysts Preparation

MnOx: A biohydrometallurgical process has been described in Gallegos *et al*. (2013). After leaching with a biogenerated sulfuric acid, the solution containing zinc and manganese were used for the synthesis of catalysts, already described in previous works. Over 100 mL of leached solution, 100 of $KMnO_4$ were added in order to react with $MnSO_4$. The solution was stirred for 30 minutes. The solid synthesized was filtered, washed with distilled water, dried at 120 ºC and calcined in air at 500 ºC during 2 hours.

https://doi.org/10.52292/j.laar.2021.193

MnZr and ***MnCe*** oxides were prepared by a co-precipitation method. $Mn(NO_3)_2 6H_2O$ and $ZrO(NO_3)_2 \cdot 2H_2O$ or $Ce(NO_3)_3 \cdot 6H_2O$ were used as precursors and were dissolved in distilled water with the molar ratio of 1:1. An aqueous solution of ammonia was used as the precipitator and was added dropwise in the metal salt solution until the pH value to 10.5. After drying at 110 ºC overnight, the solid precipitates were calcined at 500 ºC in air for 2 h.

MnCeZr oxide was prepared with the same process, usingMn$(NO_3)_2 6H_2O$, $Ce(NO_3)_3 \cdot 6H_2O$ and $ZrO(NO_3)_2 \cdot 2H_2O$ as precursors, with molar ratio of 1:0.5:0.5, respectively.

B. Characterization

Metal content were determined by atomic absorption spectrophotometry (AAS) using a Varian AA 240 spectrophotometer. Quantitative analysis of the composition of the samples were carried out with a scanning electron microscope provided with energy dispersive X-ray analysis (SEM-EDS) using a Philips SEM 505 microscope. Prepared materials have been extensively characterized using transmission electron microscopy (TEM, JEOL JEM-100CXII), temperature programmed reduction analysis (H_2-TPR), X-ray diffraction (XRD) and FTIR spectroscopy. The reduction profile (Figure 1) of the different samples was analyzed by temperature programmed reduction (H2-TPR) tests using a 5% H_2/N_2 reducing mixture carrier gas flowing at 22 cm^3 min^{-1}. The experiments were performed at a heating rate of 10 ºC min^{-1} from room temperature to 900 ºC using 50 mg of sample. Calibration was carried out with NiO. XRD was collected with a Philips PW1390 Diffractometer (CuKα radiation). Skeletal FT-IR (Fourier transform infrared spectroscopy) spectra have been recorded with a Bruker IFS66 infrared spectrometer at spectral resolution of 4 cm^{-1} accumulating 200 scans for each spectrum. The textural properties were carried using a Micromeritics Accussorb 2100 D sorptometer. Specific surface areas were obtained by BET method. Optical characterizations were carried out by measuring the diffuse reflectance spectroscopy. All spectra were taken in the range of 200-800 nm using a Perkin Elmer Lambda 35 UV-vis spectrophotometer with integrating sphere attachment and spectral on reflectance standard.

C. IR reactivity study

The surface chemistry study was performed by using Nicolet 380 FT-IR spectrometers. The catalysts were activated in the IR cell connected with conventional gas-manipulation apparatus at 773 K in air and under vacuum (10^{-4} torr). The activated samples were then contacted with chloroform vapor at room temperature (r.t) and at increasing temperatures up to 773 K. In another set of experiments, air or a mixture of air/water vapors were admitted in the IR cell together with the organic compound. Water should provide H atoms in order to favors HCl formation.

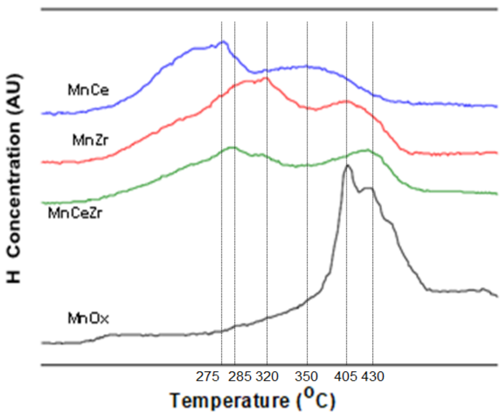

Figure 1. H_2-TPR profiles of the manganese oxides.

Table 1. BET specific area and XPS results of manganese oxides

Catalyst	SBET (m^2g^{-1})	O_{II}/O_I	Mn^{4+}/Mn^{3+}	Ce^{4+} (wt %)	Zr^{4+}/Zr^{2+}
MnO_x	37	0.67	1.85		
MnCe	83	0.66	0.39	10.8	
MnZr	249	0.58	0.69		0.75
MnCeZr	93	0.82	0.63	8.0	0.80

D. Catalytic activity

The catalytic activity of the samples in the oxidation of chloroform in air was carried out in a flow U-shape glass reactor at atmospheric pressure. 100 mg of catalyst was placed into the glass reactor and a reactive flow (2 vol % of chloroform in air) was passed through it at total flow rate of 100 cm^3 min^{-1}, which gives a gas hourly space velocity of 36000 h^{-1}. The reactants and products were measuring by GC-FID (Thermofinnigan Trace CG) together with CO_2 monitoring by an on-line detector (Telaire CO_2 sensor). The conversion of chloroform (X) and the conversion into CO_2 (XCO_2) were respectively calculated as X = {(1 – $F_{chloroform}$)/$F_{chloroform}$}, in and XCO_2 = {FCO_2/ $F_{chloroform}$} ,in where $F_{chloroform}$ is the outlet molar flow rate of chloroform at steady state, $F_{chloroform}$, in is the inlet molar flow rate of $F_{chloroform}$, FCO_2 is the outlet molar flow rate of CO_2 at steady state.

D. Results and Discussion

The sample MnOx, obtained from spent batteries, had an Mn/Zn ratio of 2.5 wt.%. The sulfur content was 2.5 wt.%. Additionally, some K was found in MnOx. The specific area of the samples is listed in Table 1together with relation between metals and types of oxygen obtained from the XPS analysis.

MnZr has the highest specific area, followed by MnCeZr, MnCe. The manganese oxide obtained from spent batteries present the lowest specific area. When analyzing the x-ray diffraction patterns they have for the sample MnOx diffraction lines corresponding to the αMnO2 phase (JCPDS 44-1386), and additionally some diffraction lines corresponding to Mn_2O_3 (JCPDS 89-4836) or $ZnMn_2O_4$ (JCPDS 71-2499) were detected. No peaks corresponding to ZnO were found. MnCe and MnCeZr present diffraction lines at 2θ = 28.1, 33.1, 48.3 and 56.7°, corresponding to CeO_2 (JCPDS 34-0394). Additionally, Mn_2O_3 is detected in MnCe, in

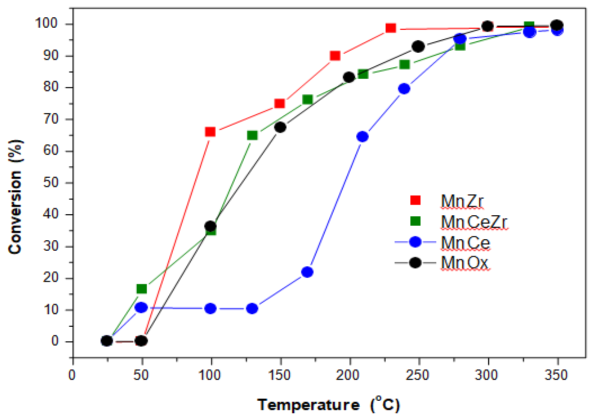

Figure 2. Chloroform conversion over catalysts in a fixed-bed flow reactor.

agreement with D´Alessandro *et al.* (2015). ZrO_2 (JCPDS 37- 1484) is the main phase present in MnCeZr, and no peaks corresponding to manganese oxide was clearly identified. Finally, Mn_2O_3 and ZrO_2 were observed in MnZr. The hydrogen temperature programmed reduction (H_2-TPR) profile for the MnOx started to be reduced at 250 ºC and display two peaks around 405 and 430ºC. This can be attributed to the reduction series MnO_2 or Mn_5O_8 - Mn_2O_3 - Mn_3O_4 – MnO (Aguilera *et al.*, 2011). In the samples prepared by coprecipitation, two broad peaks are also observed at lower temperatures than those of MnOx. The decrease in the reduction temperature of the MnCe, MnZr and MnCeZr oxides is associated to Mn–Ce and Mn-Zr interaction (D'Alessandro *et al.*, 2015; Gutiérrez-Ortiz *et al.*, 2007; Chen *et al.*, 2001). The reduction peaks are attributed to combined reduction of different components, due to the interaction among Mn, Ce and Zr in the catalysts. Among the catalysts prepared by coprecipitation, the reduction temperatures in MnCe shifted towards lower temperature compared to those of MnZr and MnCeZr, indicating that MnCe was more easily reduced. Besides, a shoulder at 225 ºC is observed in MnZr, which were assigned to nonstoichiometrically disperse MnOx phases (Gutiérrez-ortiz *et al.*, 2007). Table 1 lists the results of XPS experiments. The XPS spectra for the valence bonds of Mn $2p_{3/2}$,Zr $3d_{5/2}$ and O 1s states were recorded. The percentage of Ce was analyzed in the BE zone of 917 eV, which was assigned to Ce^{4+} (Chen *et al.*, 2001). For all the samples, the O1s peak is in general composed of three components centered at about 529, 530 and 532 eV. The lower binding energy (OI) is ascribed to lattice O, the medium binding energy peak (OII) is assigned to surface adsorbed O, OH- groups and O vacancies and the higher binding energy peak correspond to adsorbed molecular water OII species are generally considered having greater mobility than lattice oxygen (OI) and may give rise to beneficial spillover phenomena at the solid surface (Aguero *et al.*, 2011). The OII/OI ratio of the samples decrease in the following order: MnCeZr > MnOx = MnCe >MnZr. On the other hand, the Mn^{4+}/Mn^{3+} ratio of the samples diminish in the order: MnOx> MnZr > MnCeZr > MnCe.

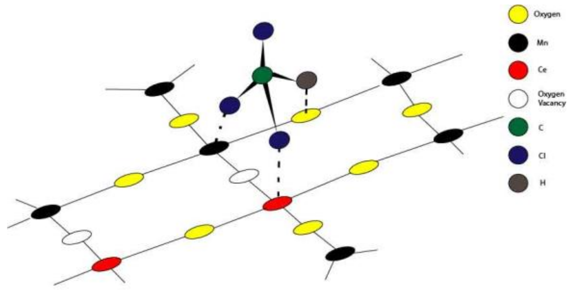

Figure 3. Proposed mechanism for the interaction of $CHCl_3$ with the catalyst surface.

Comparing the two samples containing cerium, the Ce^{4+} percentage is higher in MnCe then MnCeZr. Finally, the Zr^{4+}/Zr^{2+} ratio of the both samples containing zirconium, MnZr and MnCeZr, were 0.75 and 0.80, respectively.

Figure 2 shows the light-off curves of the chloroform decomposition over the series of Mn based catalysts. In the presence of catalysts, the only products observed were CO_2, H_2O and HCl. The T_{50} (temperature for 50% conversion) of the catalysts deceased in the order: MnZr > MnOx = MnCeZr >MnCe. Moreover, the T_{90} (temperature for 90% conversion) is also lower in MnZr than in the other three catalysts. Comparing the three manganese oxides prepared by coprecipitation, the order of conversion is similar to the order of specific surface area. The manganese oxide obtained from spent batteries, although has a lower specific area than MnCeZr and MnCe, presents a chloroform conversion similar to MnCeZr. The low surface area is compensated by a large Mn^{4+}/Mn^{3+} surface ratio. Additionally, the greater conversion observed in MnZr could be associated to the Mn-O-Zr interaction, where Mn favors the oxidation and Zr gives the acidity necessary to adsorb a Cl atom of the Cl-VOC molecule (Dobber *et al.*, 2004). In spite of the higher reducibility observed in TPR experiments of the MnCe catalyst, its low chloroform conversion could be due to the formation of CeOCl species, which could inhibit the combustion of Cl-VOCs (Rupp *et al.*, 2009). In the same way, Wang *et al.*, (2014) propose that in the oxidation of chlorobenzene over a Mn-Ce-La oxide, the adsorption-oxidation mechanism of the Cl-VOC is adsorbed by the Cl over a Ce, and the oxidation of the aromatic ring activated by Mn, being the other Cl adsorbed on the catalyst surface. According to wang's proposal, we propose for the mechanism that the Cl atoms (Fig. 3) adsorb on the Mn $^{+4}$ and Ce^{+4} and interact C and H with the oxygen atoms of the catalyst. The chlorine atoms being adsorbed on the Ce prevent the reoxidation of the network. Chloroform conversion in the absence of any catalyst did not start prior to 300 °C and reached only 20% conversion at 400 °C.

Figure 4 (A and B) shows the FTIR spectra of the oxidation of chloroform without catalyst. The formation of CO (2144 cm^{-1}), CO_2 and HCl (2887 cm^{-1}) is observed at 500 °C in the gaseous phase. In the same

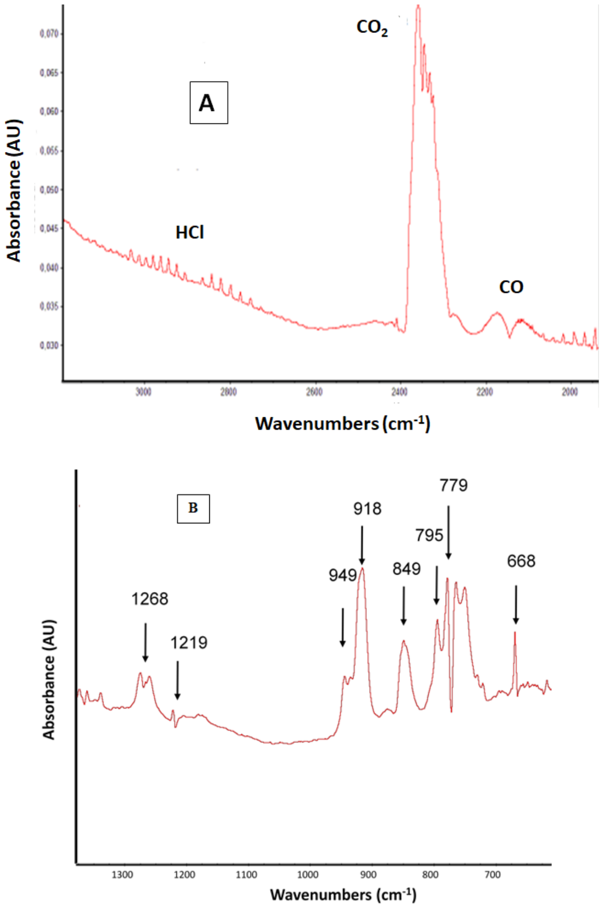

Figure 4. FT-IR spectra of gas phase arising from $CHCl_3$ combustion without catalyst at 500 °C. The gas phase at room temperature has been subtracted.

sense, bands at 1268, 1219, 949, 918, 849, 795, 779 and 668 cm^{-1} were detected. The bands at 1219 and 779 cm^{-1} are attributed to $CHCl_3$. Two bands are detected at 918 y 1268 cm^{-1}, which are assigned to CH_2Cl_2 (dichloroethane, DCE). DCE is formed by dismutation reaction (reaction 1) of $CHCl_3$, which produces DCE and CCl_4 (795 cm^{-1}, C-Cl streching). At 779 cm^{-1} is observed one band associated to tetrachloroethylene or perchloroethylene (C_2Cl_4). The formation of the different reaction products can be postulated according to

$$2CHCl_3 \rightarrow CH_2Cl_2 + CCl_4 \quad (1)$$

$$2\ CHCl_3 \rightarrow C_2Cl_4 + 2\ HCl \quad (2)$$

Below 1000 cm^{-1}, are detected three bands; one of them at 849 cm^{-1} and two bands close at 668 and 735 cm^{-1}. According to Segal Rosenheimer and Dubowski (2007) the first band is assigned to $COCl_2$ (phosgene) and the seconds could be attributed to C-Cl stretching which is associated with the formation of 1, 1, 2- trichloroethane ($C_2H_3Cl_3$, TCE).

Figure 5 (A and B) demonstrates the reaction atmosphere with MnOx catalyst. At 500 °C are detected bands at 795 cm^{-1}(CCl_4), 918 cm-1 (CH_2Cl_2) and 668 cm^{-1} (TCE), while peak at 1220 cm^{-1} corresponded to the consumption of $CHCl_3$. Between 2000 and 4000 cm^{-1} the presence of CO, CO_2 and HCl is identified.

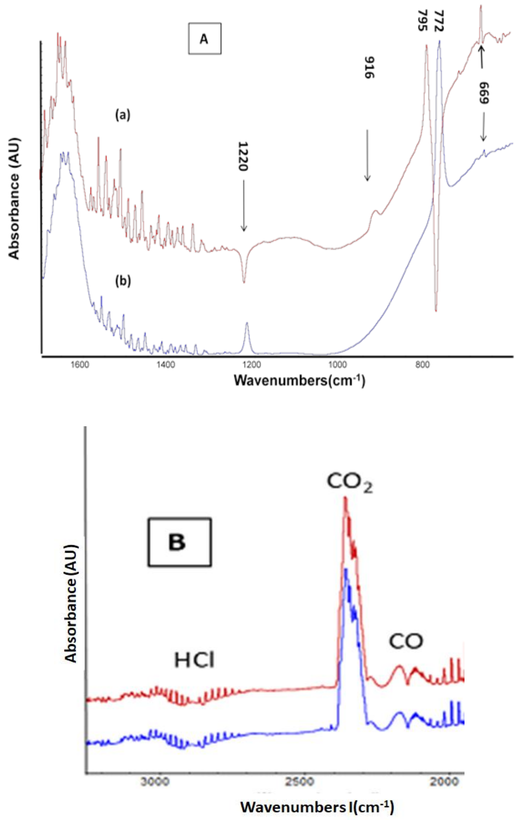

Figure 5. FT-IR spectra of gas phase arising from $CHCl_3$ combustion over MnOx sample: (A) 500 ºC, (B) 400 ºC. The gas phase at room temperature has been subtracted

Figure 6 (A and B) shows the gaseous phase of the reaction combustion of chloroform over MnZr sample. At 400 °C is observed the consumption of $CHCl_3$ and the formation of CO, CO_2 and HCl. Nevertheless, the formation of phosgene (band at 850 cm^{-1}) was determined in the reaction atmosphere. The analysis of the reaction products with catalysts allows us to say that both catalysts, MnOx and MnZr, avoided the formation of C_2Cl_4, which is a highly toxic gas. However, the presence of phosgene must be evaluated which are detected over MnZr. From the OII / OI ratio, the solid MnZr has a lower amount of reactive oxygen, so it could be said that the Mn has an oxidizing capacity and the Zr has the adsorption capacity of Cl, it favors, due to acidity, the formation of phosgene with respect to solid MnOx. Finally, Table 2 list the conversion of $CHCl_3$ at two different temperatures, 400 and 500 ºC, in the IR cell, calculated from the intensity of the $CHCl_3$ band. As it can be seen the results are similar to the catalytic activity test carried out in a fixed-bed flow reactor. Scanning electron micrographs of the MnOx, MnCe and MnZr catalysts are presented in Fig. 7. It can be seen that the catalysts show different morphological structures. MnOx sample exhibits a compact agglomerates, which are present in smaller amount on MnZr catalyst. We can suggest that Zr oxide favors the segregation of Mn over the catalyst surface and ZrO_2 improves the acidity of the catalyst due to the formation of Brønsted acid sites (Gao *et al*., 2013). However, the results

Table 2. $CHCl_3$ conversion (%) at 400 and 500 ºC calculated in the IR cell and T_{50} and T_{90} values of the $CHCl_3$ oxidation obtained in the fixed-bed flow reactor

catalyst	IR X_{CHCl3} (%)		Fixed-bed flow reactor	
	400 ºC	500ºC	400ºC	500ºC
MnOx	78	96	122	240
MnCe	41	70	194	269
MnZr	72	91	87	200
MnCeZr	76	91	116	267
blank		37		

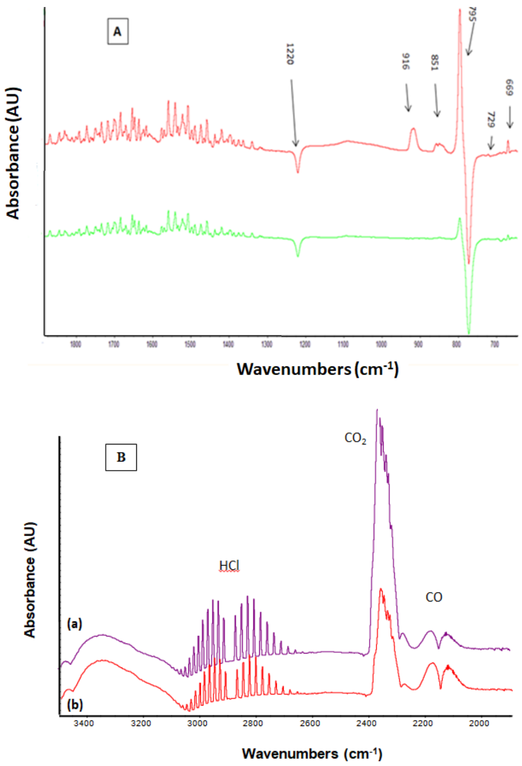

Figure 6. FT-IR spectra of gas phase arising from $CHCl_3$ combustion over MnZr sample: (a) 500 ºC, (b) 400 ºC. The gas phase at room temperature has been subtracted.

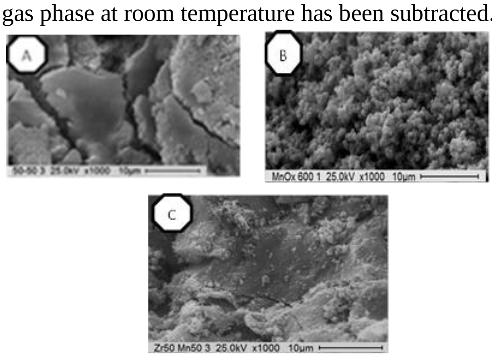

Figure 7. Scanning electron micrographs of the catalysts. MnCe (A), MnOx (B) and MnZr (C)

showed that the combustion of chloroform over MnZr has favored the formation of phosgene, obtaining similar results for the MnCeZr catalyst.

III. CONCLUSIONS

The catalytic performance of a series of Mn-based catalysts (MnCe, MnZr and MnCeZr) was examined for the gas-phase oxidation of chloroform. The samples were compared with a manganese oxide obtained from spent batteries (MnOx). The chloroform conversion in the fixed bed reactor follows the order:MnZr > MnOx = MnCeZr >MnCe. The conversion is related to the specific surface area and the Mn^{4+}/Mn^{3+} superficial ratio. The Mn-Zr interaction favors the chloroform conversion, whereas Ce has a detrimental effect on the conversion. In situ IR studies showed that in the absence of catalysts, CCl_4, $COCl_2$ (phosgene), C_2Cl_4 and CH_2Cl_2, which are harmful species, were detected. In the presence of catalysts, $CHCl_3$ is oxidized at lower temperatures and the formation of C_2Cl_4 is avoided. In spite of this, CCl_4 and CH_2Cl_2 were observed.

REFERENCES

Aguero, F.N., Barbero, B.P., Costa-Almeida, L., Montes, M., and Cadús, L.E. (2011) MnOx supported on metallic monoliths for the combustion of volatile organic compounds. *Chem. Eng. J*. **166,** 218–223.

Aguilera, D.A., Perez, A., Molina, R., and Moreno, S. (2011) Cu-Mn and Co-Mn catalysts synthesized from hydrotalcites and their use in the oxidation of VOCs. *Appl. Catal. B Environ*. **104**, 144–150.

Ahn, C.W., You, Y.W., Heo, I., Hong, J.S., Jeon, J.K., Ko, Y.D., Kim, Y.H., Park, H., and Suh, J.K. (2017) Catalytic combustion of volatile organic compound over spherical-shaped copper–manganese oxide. *J. Ind. Eng. Chem*. **47**, 439–445.

Baldi, M., Finocchio, E., Milella, F., and Busca, G. (1998) Catalytic combustion of C_3 hydrocarbons and oxygenates over Mn_3O_4. *Appl. Catal. B Environ*. **16**, 43–51.

Belkouch, J., Ould-Dris, A., and Taouk, B. (2009) Removal of hazardous chlorinated VOCs over Mn-Cu mixed oxide based catalyst. *J. Hazard. Mater*. **169**, 758–765.

Biswas, R.K., Karmakar, A.K., and Kumar, S.L. (2016) Recovery of manganese and zinc from spent Zn–C cell powder: Experimental design of leaching by sulfuric acid solution containing glucose. *Waste Manag*. **51**, 174–181.

Carabineiro, S.A.C., Chen, X., Konsolakis, M., Psarras, A.C., Tavares, P.B., Órfão, J.J.M., Pereira, M.F.R., and Figueiredo, J.L. (2015) Catalytic oxidation of toluene on Ce–Co and La–Co mixed oxides synthesized by exotemplating and evaporation methods. *Catal. Today*. **244**, 161–171.

Chen, H., Sayari, A., Adnot, A., and Larachi, F. (2001) Composition–activity effects of Mn–Ce–O composites on phenol catalytic wet oxidation. *Appl. Catal. B Environ*. **32**, 195–204.

Cho, W.C., Poo, K.M., Mohamed, H.O., Kim, T.N., Kim, Y.S., Hwang, M.H., Jung, D.W., and Chae, K.J. (2018) Non-selective rapid electro-oxidation of persistent, refractory VOCs in industrial wastewater using a highly catalytic and dimensionally stable Ir–Pd/Ti composite electrode. *Chemosphere*. **206**, 483–490.

Colman-Lerner, J.E., Peluso, M.A., Sambeth, J.E., and Thomas, H.J. (2016) Cerium, manganese and cerium/manganese ceramic monolithic catalysts. Study of VOCs and PM removal. *J. Rare Earths*. **34**, 675–682.

D'Alessandro, O., Sathicq, Á.G., Sambeth, J.E., Thomas, H.J., and Romanelli, G.P. (2015) A study of the temperature effect on Hantzsch reaction selectivity using Mn and Ce oxides under solvent- free conditions. *Catal. Commun*. **60**, 65–69.

De Rivas, B., López-Fonseca, R., Gutierrez-Ortiz, M.A., Gutiérrez-Ortiz, J.I. (2008) Analysis of the behaviour of different mixed oxides in the treatment of Cl-VOC containing gas streams. *Int. J. Chem. React. Eng.* **6**, A47.

Dobber, D., Döbber, D., Kießling, D., Schmitz, W., and Wendt, G. (2004) MnOx/ZrO_2 catalysts for the total oxidation of methane and chloromethane. *Appl. Catal. B Environ*. **52**, 135–143.

Gallegos, M.V., Falco, L.R., Peluso, M.A., Sambeth, J.E., and Thomas, H.J. (2013) Recovery of manganese oxides from spent alkaline and zinc-carbon batteries. An application as catalysts for VOCs elimination. *Waste Manag*. **33**, 1483–1490.

Gallegos, M.V., Peluso, M.A., Finocchio, E., Thomas, H.J., Busca, G., and Sambeth, J.E. (2017) Removal of VOCs by catalytic process. A study of MnZnO composites synthesized from waste alkaline and Zn/C batteries. *Chem. Eng. J*. **313**, 1099–1111.

Gao, R., Zhang, D., Maitarad, P., Shi, L., Rungrotmongkol, T., Li, H., Zhang, J., and Cao, W. (2013) Morphology-dependent properties of MnOx/ZrO_2-CeO_2 nanostructures for the selective catalytic reduction of NO with NH_3. *J. Phys. Chem. C*. **117**, 10502–10511.

Genuino, H.C., Dharmarathna, S., Njagi, E.C., Mei, M.C., and Suib, S.L. (2012) Gas-phase total oxidation of benzene, toluene, ethylbenzene, and xylenes using shape-selective manganese oxide and copper manganese oxide catalysts. *J. Phys. Chem. C*. **116**, 12066–12078.

Granger, P., Parvulescu, V.I., Kaliaguine, S., and Prellier, W. (2016) *Perovskites and Related Mixed Oxides: Concepts and Applications*. Wiley-VCH, Weinheim, Germany.

Gutiérrez-Ortiz, J.I., De Rivas, B., López-Fonseca, R., Martín, S., and González-Velasco, J.R. (2007) Structure of Mn-Zr mixed oxides catalysts and their catalytic performance in the gas-phase oxidation of chlorocarbons. *Chemosphere*. **68,** 1004–1012.

Jose, J., Ramanujam, S., and Philip, L. (2018) Applicability of pulsed corona discharge treatment for the degradation of chloroform. *Chem. Eng. J*. **360,** 1341-1354.

Lou, J.C., and Chang, Y.S. (1997) Thermal oxidation of chloroform. *Combust. Flame*. **109**, 188–197.

Rodríguez-Chueca, J., Mediano, A., Pueyo, N., García-Suescun, I., Mosteo, R., and Ormad, M.P. (2016) Degradation of chloroform by Fenton-like treatment induced by electromagnetic fields: A case of study. *Chem. Eng. Sci*. **156**, 89–96.

Rossin, J.A. and Farris, M.M. (1993) Catalytic oxidation of chloroform over a 2% platinum alumina catalyst. *Ind. Eng. Chem. Res*. **32**, 1024–1029.

Rupp, E.C., Betterton, E.A., Arnold, R.G., and Sáez, A.E. (2009) Interaction of perchloroethylene with cerium oxide in three-way catalysts. *Catal. Letters*. **132**, 153–158.

Segal-Rosenheimer, M., and Dubowski, Y. (2007) Heterogeneous ozonolysis of cypermethrin using real-time monitoring FTIR techniques, *J. Phys. Chem. C*. **111**, 11682–11691.

Wang, X., Ran, L., Dai, Y., Lu, Y., and Dai, Q. (2014) Removal of Cl adsorbed on Mn-Ce-La solid solution catalysts during CVOC combustion. *J. Colloid Interface Sci*. **426**, 324–332.

Received: September 3, 2019
Sent to Subject Editor: October 11, 2019
Accepted: October 25 2020
Recommended by Subject Editor Maria Luján Ferreira